

Methane adsorbed on graphite. III. The bilayer and trilayer

James M. Phillips

Department of Physics, University of Missouri—Kansas City, Kansas City, Missouri 64110-2499

(Received 17 January 1986)

Models for the monolayer, bilayer, and trilayer of methane (CH_4 and CD_4) adsorbed on the basal plane of graphite are studied using the quantum-mechanical cell model. The calculations are made for a range of temperatures from the ground state to near the two-dimensional triple line. This microscopic finite-temperature model gives quantitative results for structural and thermodynamic properties. The results include the following: the equilibrium structure for the system, the conditions for monolayer-bilayer and bilayer-trilayer coexistence, comparisons to three-dimensional bulk solids, incommensurability to the substrate, and the chemical potential for the entire temperature range for a stable solid film. The results show that the bilayer and trilayer films are significantly compressed at coexistence. The planar nearest-neighbor distance (at coexistence) is less than that of the corresponding bulk solid. However, the chemical potential of the film is still below that of bulk value.

I. INTRODUCTION

The goal of this investigation is to study, in microscopic detail, the structural and thermodynamic properties of solid monolayer, bilayer, and trilayer films of methane adsorbed on the basal plane of graphite. In extending recent potential energy¹ and low-temperature calculations,² this investigation uses statistical mechanics to include finite-temperature effects spanning nearly the entire range of the stable solid film.

Multilayer growth and wetting phenomena are currently the subject of much vigorous activity. A variety of experimental techniques and general theoretical models have given definition to a number of layer-growth regimes and phase diagrams. The new activity has been a natural consequence of the earlier work in physical adsorption and recent work in the physics of two dimensions. The additional complexities in the growth of physisorbed systems in a third dimension (vertical) creates the need for an extension of computational methodologies.

There are serious problems in making comparisons between the clear quantitative experimental results and the predictions of simplified theoretical models which have enough breadth to reveal the great variety of features contained in the phase diagrams. On the other hand, quantitative calculations seldom have the precision required to study critical phenomena and to demonstrate the universal character of a class of systems.

Computational approaches to the problem need to be developed with the approximations consistent with the region of the phase diagram for which experimental data exists. The methods that follow are an attempt to do this in the range of temperatures and densities of solid monolayer, bilayer, and trilayer films.

The calculations apply to wetting phenomena only under the assumption that the character of the growth to bulk is established in the adsorption of the first two or three layers. In this way, some insight into the transition

from a two-dimensional to a three-dimensional system may be gained at the microscopic level.

The literature on multilayer growth has been well reviewed elsewhere.³ It is sufficient to say that experiments using electron, x-ray, and neutron diffraction, thermodynamic techniques, and nuclear magnetic resonance studies have all contributed greatly to the present understanding of low-temperature solid films. Experiments, as reviewed by Bienfait,³ are summarized by noting that of the more than two dozen physisorbed low-temperature films, all (including methane) have shown "incomplete wetting" (type 2, Stranski-Krastanov) modes of layer growth except Xe, Kr, and Ar adsorbed on graphite (complete wetting, type 1, Frank—van der Merwe).

In terms of its physical parameters, methane is intermediate to argon and neon, and is therefore an important system to study theoretically. The bilayer properties of argon on graphite⁴ and neon on graphite⁵ have been studied. Comparisons with this work permit several proposed mechanisms for multilayer growth to be investigated.

In previous work,⁶ hereafter referred to as papers I and II, an interaction model and a computational technique were successful in predicting a number of experimental results. This paper reports the extension of the calculations to three dimensions and the addition of a second and a third layer to the film. The individual layers of the bilayer and trilayer are treated separately in order that the elastic strain between them while at equilibrium in the multilayer structure can be determined.

The thermodynamic conditions for a multilayer at equilibrium are given in Sec. II. Section III is an outline of the intermolecular and molecular-substrate models used in this investigation. The quantum cell model, the calculation of the Helmholtz free energy, and the Gibbs free-energy constructions for multilayer coexistence are given in Sec. IV. Section V is a presentation of the quantitative results. A discussion of this model of multilayer growth is offered in Sec. VI.

II. THERMODYNAMIC EQUILIBRIUM OF ADSORBED LAYERS

This paper is a report of the relevant thermodynamic properties along three boundaries in the solid region of the phase diagram. These points are indicated in Fig. 1, a schematic of a possible multilayer phase diagram. The first boundary of interest is the two-dimensional (2D) sublimation line. Along this line, the uncompressed solid monolayer is in equilibrium at essentially zero spreading pressure. The next indicated boundary is for the completed and compressed solid bilayer. This boundary is determined by a free-energy diagram for the coexistence of a monolayer and bilayer. In the same manner, at even higher spreading pressures, the next boundary is the coexistence line for the bilayer with the trilayer. This could go on until a very thick film is essentially three-dimensional (3D) bulk. If the coexistence conditions with the 3D bulk are approached in a monotonic sequence as the number of layers goes to infinity, the process is called wetting. If bulk conditions are met in with a finite number of layers (≥ 1), the process is called partial wetting (see Krim, Ref. 3). The discussion below is restricted to three layers. In light of the difficulty of growing stable bilayers and trilayers experimentally, the results should be informative. Gittes and Schick⁷ discuss both growth modes for a very large number of layers using potential energy models.

This study involves the calculation of the Helmholtz free energy for a quantitative model which includes a detailed molecular description, zero point effects, substrate mediated forces, and the influences of temperature over the range of the stable two-dimensional solid. The proper thermodynamic functions for this model are the chemical potentials for the coexisting phases. For these reasons, the equilibrium conditions derived by Bruch⁴ are used over those of Gittes and Schick.⁷ The thermodynamic potential of Gittes and Schick, while proper for their calculation, does not include explicitly the dynamical contribution for finite temperatures. The chemical potential, as a natural function of temperature and pressure, is necessary when calculating the thermodynamic properties of coexisting solid films over a temperature range. The equilibrium conditions for this model⁴ are a consequence of these working variables.

At low temperatures, the calculation of the thermodynamic properties of successive layer-by-layer growth (see Fig. 2) of very thin solid films is computationally simpler than for fluids or partial layers. The contribution to the total energy by the interaction of the film with the 3D gas is quite small and the statistical mechanics of the solid adsorbate is amenable to well understood approximations.

Defining the variables to agree with the original derivation by Bruch⁴ gives the area per molecule in a j layer to be

$$a_j = \sqrt{3/4} L_j^2 / j,$$

where L_j is the nearest-neighbor distance in a layer plane. The height of the bottom layer of a j layer above the substrate is l_j and the distance between the i and $i + 1$ layers within a j layer is $z_{i, i+1}$. The Helmholtz free energy per

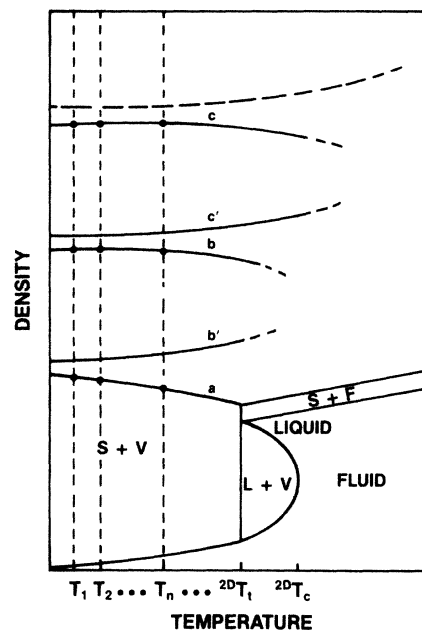


FIG. 1. A schematic of a multilayer phase diagram. The branches a , b , and c represent the monolayer, bilayer, and trilayer solids, respectively, at coexistence. The data in Tables II–VI have been calculated at the different temperatures indicated by the closed circles. The lower part of the diagram is for a 2D system.

molecule of a j layer is

$$f_j = f_j [T, a_j, l_j, (z_{i, i+1})].$$

The constraints on the coexisting j - and $(j + 1)$ -layer structures are the total adsorbing area

$$A = N_j a_j + N_{j+1} a_j \quad (1)$$

and the number of adsorbed molecules

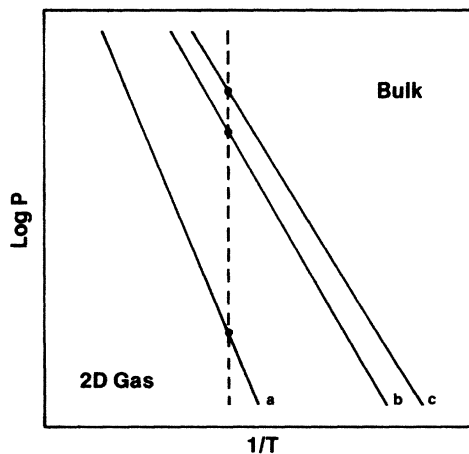


FIG. 2. A schematic of a multilayer phase diagram as a function of the 3D gas pressure and the reciprocal temperature. Lines a , b , and c are the monolayer, bilayer, and trilayer branches, respectively. The dashed line shows the points of the growth of successive layers at a constant temperature with increasing 3D gas pressure.

$$N_A = N_j + N_{j+1}, \quad (2)$$

where N_j is the number of molecules in a j layer.

The equilibrium coexistence conditions of a j layer with a $j+1$ layer are found by minimizing the Helmholtz free energy of the system,

$$F_A = N_j f_j(T, a_j, l_j, \{z_{i, j+1}\}) + N_{j+1} f_{j+1}(T, a_{j+1}, l_{j+1}, \{z_{i, j+1}\}), \quad (3)$$

subject to the constraints Eqs. (1) and (2).

The spreading pressure of a j layer is

$$\phi_j = - \frac{\partial f_j}{\partial a_j} \quad (4)$$

and the chemical potential is

$$\mu_j = f_j + a_j \phi_j. \quad (5)$$

The conditions are

$$\mu_j = \mu_{j+1} \quad (6)$$

and

$$\phi_j = \phi_{j+1}. \quad (7)$$

The vertical dimensions of the structure are found by searching for the conditions

$$\frac{\partial f_j}{\partial l_j} = 0, \quad \frac{\partial f_{j+1}}{\partial l_{j+1}} = 0, \quad (8)$$

and

$$\frac{\partial f_{j+1}}{\partial z_{j, j+1}} = 0.$$

The latent heat of adsorption of the bilayer at coexistence is⁸

$$q_2 = 4k_B T - [(a_1 u_2 - a_2 u_1)/(a_1 - a_2)], \quad (9)$$

where u_j is the internal energy per molecule of the j layer. For inert gases, the ideal-gas enthalpy is $\frac{5}{2}k_B T$ rather than the first term of Eq. (9) where the orientational degrees of freedom are included. For the monolayer at $\phi=0$, the latent heat of adsorption is given,

$$q_1 = 4k_B T - u_1, \quad (10)$$

while holding the vertical structure parameters constant.

The difference between the isosteric heat and q_1 is a measure of the contribution of lateral interactions to the monolayer at three-phase coexistence,⁸

$$q_{st} - q_1 = \frac{1}{2} L \left[\frac{\partial u}{\partial L} \right]_T, \quad (11)$$

where L is the nearest-neighbor distance of the 2D crystal and u is the lateral internal energy per atom. The lateral isothermal compressibility is

$$K_{T, j+1} = - \left[\frac{1}{a_{j+1}} \right] \left[\frac{\partial a_{j+1}}{\partial \phi_{j+1}} \right] \Bigg|_{T, l, \{z_{i, j+1}\}}. \quad (12)$$

III. INTERACTION MODELS

The prediction of the macroscopic properties of condensed systems from realistic interaction models of their microscopic constituent particles is a basic goal of theory. However, precise interaction potentials are very rare, with the exception of the inert gases.^{9,10} For small molecules, several less accurate atom-atom intermolecular potentials have been suggested.¹¹ Models for methane have been revised several times to give at least one that is a reasonable scaling of the methane-methane and methane-graphite interactions.¹² A number of properties are approximated moderately well by this potential.⁶ When comparisons are made internal to the model, e.g., film to bulk, the model represents several features observed in experiments. Within limits, these quite empirical potentials can give insights into molecular systems, providing the parameters have been tested over many different properties and good fortune accompanies their successive revisions. An example can be drawn from the compromises that are made in the set of parameters used in the calculations that follow. The influence of methane's octapole moment is assimilated into these "effective" parameters, but in the models used by O'Shea and Klein¹³ and Righini *et al.*¹⁴ it is given explicitly. In the few cases where comparisons can be made between the potentials, the results are similar.

The calculations reported in the next section require the detailed characterization of two different potential models, methane-methane for interactions internal to the adsorbate, and methane-graphite for the interaction of the adsorbate to the substrate. The interaction models are used to build a cylindrically symmetric, three-dimensional, anharmonic cell potential (see Fig. 3). Solving for the quantum-mechanical energy levels in this cell potential is the basis for the statistical mechanics of the multilayers of methane adsorbed on graphite.

The methane-methane and the methane-graphite interactions are taken to be Lennard-Jones, LJ(12,6), atom-atom pair potentials with parameters given by Severin and Tildesley¹² and used in papers I and II of this series⁶ (see

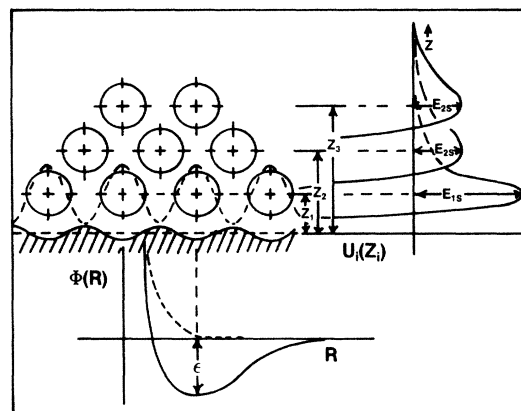


FIG. 3. A representation of a trilayer solid above a low-amplitude periodic substrate. A schematic of the Steele potential for the methane-graphite and the methane-methane interactions is on the right. The pair (solid) with the MacLachlan (dashed) potentials is shown below.

TABLE I. The parameters of the Lennard-Jones (12,6) atom-atom interaction. This table is from the study of Serevin and Tildesley (Ref. 12).

Interaction	ϵ_{ij}/k_B (K)			σ_{ij} (Å)		
	I ^a	II ^b	III ^c	I ^a	II ^b	III ^c
CH ₄ -CH ₄						
C _m -C _m	51.198	47.68	51.198	3.35	3.35	3.35
C _m -H _m	27.798	24.46	23.798	2.995	2.99	2.99
H _m -H _m	8.631	4.87	4.87	2.813	3.12	2.61
Graphite						
C _g -C _g	28.00			3.40		
CH ₄ -graphite						
C _g -C _m	37.862	47.68	47.68	3.375	3.35	3.30
C _g -H _m	15.54	24.46	17.00	3.107	2.99	2.98

^aFrom dense fluid methane data.

^bFrom the Williams study (Ref. 11).

^cFrom the adjusted set by Severin and Tildesley (the set used in the present work).

Table I). Lattice sums are calculated for a methane molecule in a solid adsorbate film and over a semi-infinite graphite substrate. The results of these sums are then used to characterize a spherically symmetric methane molecule with a LJ(12,6) potential ($\epsilon/k_B=137$ K and $\sigma=3.6914$ Å). Additional sums set the parameters for a Steele, $\Sigma(4-10)$ potential¹⁴ for the adsorbate-substrate potential $u(z)$. This expression is incorporated into the vertical cell potential. Utilized in this way, the following relationships are merely the analytic forms fitted to the results of the atom-atom lattice sums. The adsorbate-substrate potential for a molecule at height z above the graphite surface is approximated by

$$u(z) = \epsilon_{1s} \sum_{j=0} \left[\frac{2}{3} \left(\frac{\sigma_{gs}}{z+jd} \right)^{10} - \left(\frac{\sigma_{gs}}{z+jd} \right)^4 \right], \quad (13)$$

where $\epsilon_{1s}/k_B=1468.5$ K, $\sigma_{gs}=3.297$ Å, and $d=3.37$ Å. The same form is used to represent the vertical component of the interaction of an i th layer of the adsorbate to the cell potential of a j th layer molecule, $u(z_{ij})$. For one layer to another, $\epsilon_{2s}/k_B=612.94$ K and $\sigma_{g2}=3.28$ Å. For the top layer of the trilayer to the two below, $\epsilon_{3s}/k_B=653.42$ K and $\sigma_{g3}=3.28$ Å. The upper limit of the sum in Eq. (13) is for an infinite number of graphite planes in the first case but only over one or two layers in the case of the film. The z_{ij} scanned for a minimum in the Helmholtz free energy for the full calculation at all relevant temperatures. Steele has given polynomial approximations for these potentials.¹⁵ Computational efficiency is greatly improved by his approximations.

The lateral interactions involve a small but significant effect from the periodic nature of the substrate or adjacent layer adsorbate potential. In the case of a monolayer, the low-temperature ordering to a $\sqrt{3} \times \sqrt{3}$ structure is direct evidence of the effect. The amplitude of the periodic potential of methane over methane is an order of magnitude greater than that for methane over graphite. The potential used for the substrate periodicity (either graphite or other methane layers) is again a formula by Steele.¹⁶

The substrate potential is given by

$$V(r,z) = \sum_{G_j} V_{G_j}(z) \exp(i\mathbf{G}_j \cdot \mathbf{r}).$$

The constants are determined by lattice sums over the graphite in the first case and over the other layers of methane in the second. For both a middle layer of methane in a trilayer or a first layer, in either a bilayer or trilayer, the periodicity is felt from above as well as below. The stacking is assumed to be *ABA* for the trilayer case.

Substrate mediated interactions¹⁷ are included in the cell potential for the following calculations. The largest of these is the MacLachlan¹⁸ interaction. The energy of two adsorbate molecules at a distance r and both at a height L above the substrate is

$$\Phi_M(r) = C_{s1} \left[\frac{4}{3} - 4L^2/(r^2+4L^2) \right] / [r(r^2+4L^2)^{1/2}]^3 - C_{s2}/(r^2+4L^2)^3. \quad (14)$$

For the methane-on-graphite system,¹⁹ $C_{s1}=4.360 \times 10^5$ K/Å (Ref. 6) and $C_{s2}=2.301 \times 10^5$ K/Å (Ref. 6). Surface dipoles are believed to be small and are excluded from the calculations. The Axilrod-Teller-Muto triple dipole interaction is included in the film energy with the coefficient given by Margoliash *et al.*²⁰

IV. FINITE TEMPERATURE CALCULATIONS

The computational methodology use in this study is indicated by both the physics of the systems investigated and the thermodynamic details sought. A finite-temperature modeling of methane on graphite requires a statistical mechanics approach in order to quantitatively describe the conditions in which monolayers, bilayers, and trilayers exist in laboratory environments. This model is an attempt to extend the earlier studies using lattice-gas assumptions by considering scaled intermolecular potential functions (see Pandit *et al.* in Ref. 3) and allowing the particles of the system to have continuous translational freedom. Incorporating dynamical properties over a range

of finite temperatures permits more direct comparisons of the calculated results with experiments. With the above effects considered to a good approximation by available methods, the first few stages of multilayer-growth modes are studied over the range of temperatures needed for solid films. The methods are sufficiently broad to allow the calculation of a variety of thermodynamic properties for the multilayers at coexistence.

Solid films of methane on graphite have two important characteristics that require consideration, quantum effects and anharmonicity.²¹ Quantum effects have been shown to alter significantly the thermal properties of 2D neon and to slightly affect 2D argon.²¹ The deBoer parameter²² is given by

$$\Lambda^* = 2\pi\hbar / [\sigma(m\epsilon)^{1/2}]$$

for a system with atomic mass m , Lennard-Jones parameters σ , ϵ , and reduced Planck constant \hbar . The deBoer parameter for argon is 0.186 and for neon it is 0.576. Methane (CH_4) has a deBoer parameter 0.245 and the deuterated molecule (CD_4), 0.219. These values are intermediate to neon and argon. Previous experiments have shown argon to have a uniform layer-by-layer growth mode (wetting). Whereas the case for neon is controversial, experiment shows growth to bulk after one layer (partial wetting),²³ and calculation indicates that the first three grow uniformly.²⁴ The isotopes of methane are intermediate to neon and argon. They provide a natural system to investigate the range of deBoer parameter between neon and argon.

Quasiharmonic lattice dynamics²⁵ gives a reasonable approximation to the thermodynamic properties of argon at very low temperatures but produces sizable errors above $T=20$ K (see Figs. 2–4 in Ref. 21). The same calculation for neon parameters shows some disagreement at zero temperature and increasingly significant errors above the ground state. In order to transcend these limitations, cell theory is utilized to cover the temperatures of interest and account for the highly anharmonic nature of the potentials. The quantum-mechanical version of cell theory is necessary²¹ for systems with deBoer parameters in the range of neon and methane. It is, of course, not adequate for helium. Quantum-mechanical cell theory (QCT) has been developed²¹ and applied⁶ to physisorbed systems. Classical cell theory has been reviewed by Barker.²⁶ Quantum-corrected cell theory has been discussed by Phillips and Bruch²⁵ and applied to solid films by Bruch and Wei.⁴ Cell theory was tested with computer simulations in 3D (Ref. 27) and 2D (Ref. 28).

The quantum-mechanical cell model is formulated for a three-dimensional structure of independent Einstein oscillators in a cylindrically symmetric cell potential that is quite anharmonic. The cell potential is constructed from the potentials outlined in the preceding section. A more detailed account is given in Ref. 21. The cell potential is a quite realistic representation of the potential well for a methane molecule in an adsorbed film. The potential represents the presence of a semi-infinite graphite substrate with triangular array of adsorbate molecules in a parallel plane (see Fig. 3). Monolayer, bilayer, and trilayer films are taken to be *ABA* stackings of additional planes

of molecules.

The 3D cell potential $\omega(r,z)$ is a superposition of the lateral interactions of in-plane neighbors (36 shells) with the vertical potential $u(z)$ of the substrate and other adsorbate layers. The lateral interaction from other layers are added to the cell potential from the periodic Steele potential.¹⁶ The periodic nature of the layers above and below, as well as that of the substrate are included in the composition of the cell potential. The composite potential becomes the potential-energy term in the single-particle Schrödinger equation.

A system of N adsorbed molecules of mass m and with pair interactions ϕ in the film and ϕ' for the molecule-substrate, has a Hamiltonian

$$H = \sum_{i=1}^N p_i^2/2m + \frac{1}{2} \sum_{\substack{i,j=1 \\ i \neq j}}^N \phi(|\mathbf{R}_i + \mathbf{r}_i - \mathbf{R}_j - \mathbf{r}_j|) + \frac{1}{2} \sum_{\substack{i,k=1 \\ i \neq k}}^N \phi'(|\mathbf{R}_i + \mathbf{r}_i - \mathbf{R}_k - \mathbf{r}_k|), \quad (15)$$

where the j index runs over the adsorbate neighbors and the k index over the substrate atoms. The cell potential is the cylindrically averaged energy of a molecule (i) in the field of its fixed neighbors (j) film and (k) substrate:

$$\omega(r,z) = \sum_j [\overline{\phi(|\mathbf{R}_i + \mathbf{r} - \mathbf{R}_j|)} - \phi(R_{ij})] + \sum_k [\overline{\phi'(|\mathbf{R}_i + \mathbf{r} - \mathbf{R}_k|)} - \phi'(R_{ik})]. \quad (16)$$

The Hamiltonian is rewritten with the cell potential

$$H = (N/2) \sum_{\substack{j=1 \\ j \neq i}}^N \phi(R_{ij}) + (M/2) \sum_{\substack{k=1 \\ k \neq i}}^N \phi'(R_{ik}) + \sum_{i=1}^N [p_i^2/2m + \omega(r_i,z)] + \Delta. \\ = H_0 + \Delta. \quad (17)$$

The Δ term is the difference between the sum of the pair potentials in Eq. (15) and the static lattice sum plus the cell potential. This term is dropped in the following calculations. A self-consistent cell model²⁹ would include this term and give the correct entropy. This calculation is missing the communal entropy associated with these correlational effects. For solids, the missing entropy is small. It can be partially recovered by a harmonic approximation.^{28,30}

The thermodynamic properties are obtained from the partition function

$$Z = \text{Tr} e^{-\beta H_0}, \quad (18)$$

where $\beta = 1/(k_B T)$, k_B is the Boltzmann constant, T is the absolute temperature, and Tr denotes the trace found by a sum over the eigenstates of the H_0 .

The Schrödinger equation,

$$H_0 \psi(r,z) = E \psi(r,z), \quad (19)$$

is expressed in cylindrical coordinates for the separation

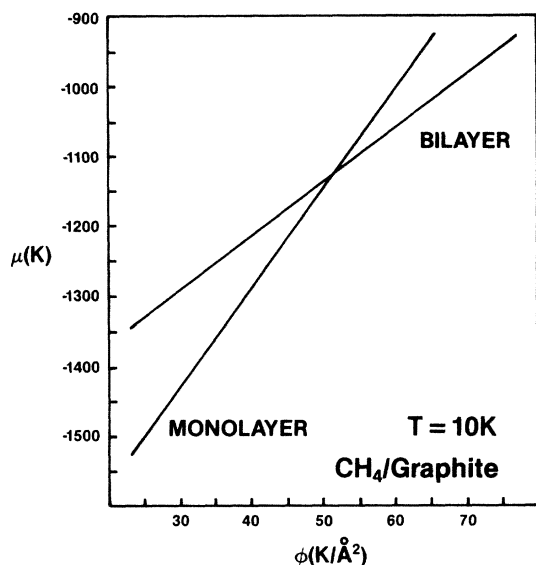


FIG. 4. A graph of the chemical potential diagram as a solution for the coexistence conditions of monolayer-bilayer solid films. The data represented is for a temperature of 10 K.

of variables and solved numerically²¹ for the energy eigenvalues. The Helmholtz free energy per particle is

$$F/Nk_B = -T \ln Z \quad (20)$$

and the specific heat at constant volume is given by

$$C/Nk_B = [1/(k_B T)^2] (\langle E^2 \rangle - \langle E \rangle^2). \quad (21)$$

The isothermal compressibility K_T can be calculated by numerical derivatives of the Helmholtz free energy with respect to volume. Table II shows some of the typical values for the energy eigenstates found in the CH_4 and CD_4 on graphite systems.

The next step in the calculation is to find, at a given temperature, the equilibrium structure of the monolayer. By varying the dilation of the planar lattice and, separately, the height of the monolayer above the substrate, the minimum Helmholtz free energy can be found (zero spreading pressure). For the bilayer and trilayer structures, the vertical separations of all the layers are varied to

again find a minimum in the Helmholtz free energy. The lateral lattice constant (nearest-neighbor distance in a layer plane) is also systematically scanned for each layer separately to considerable compression. The chemical potential is calculated from the Helmholtz free energy and the spreading pressure in Eq. (5). With decreasing dilation, the chemical potential is plotted versus the spreading pressure for the monolayer and bilayer (see Fig. 4). At the intersection of these nearly straight line plots, the coexistence conditions Eqs. (6) and (7) are met. The same procedure is followed for the bilayer-trilayer coexistence conditions. The calculation is repeated for all of the temperatures of interest.

V. RESULTS

The results of these calculations give quantitative information on the equilibrium structures, thermodynamic properties, and multilayer transitions of solid films of CH_4 and CD_4 on graphite. The following data is directly from the interaction potentials outlined in Sec. III. The empirical potentials for the methane on graphite system in the original work of Severin and Tildesley¹² and papers I and II of this series are a qualified success. The representation of the system used here appears to be a reasonable compromise. Recent experiments by Gay *et al.*³¹ have shown good agreement with several of the predictions of I and II over those of an earlier model.³² Although the comparisons are often quite good, the most valuable uses to be made of these results are the relative comparisons within the model.

The structure of the monolayer was given in paper II (Ref. 6) except for the dynamical contribution to the height above the graphite. Static lattice sums give the methane monolayer to be 3.32 Å above the graphite and the quantum-cell model gives 3.28 Å. Vertical thermal expansion is less than 0.01 Å from 0 to 60 K. Adding the second layer to form the bilayer compresses the first layer height to 3.24 Å and the equilibrium height for the second layer is 6.50 Å above the graphite. The trilayer vertical heights are the same as the bilayer with the third layer at 9.74 Å. The thermal expansion in the z direction is again very slight over 0 to 60 K and would not be detectable by

TABLE II. Examples of the quantum-mechanical energy levels. The ground state and the first two excited states are given for CH_4 /graphite. The units are given in degrees kelvin. The levels are given as the energy above the bottom of the potential energy well. The films are in their respective coexisting states. The temperature was 10 K and the lattice constants are given in Table III. The angular momentum quantum number of the lateral states is zero for the examples given.

Monolayer		Bilayer (first)		Bilayer (second)	
Vertical	Lateral	Vertical	Lateral	Vertical	Lateral
65.627	56.779	57.595	91.286	44.747	89.423
191.078	181.475	164.860	285.242	128.234	280.020
308.991	322.126	261.791	496.012	204.400	487.858
Trilayer (first)		Trilayer (second)		Trilayer (third)	
Vertical	Lateral	Vertical	Lateral	Vertical	Lateral
56.833	96.336	43.555	95.644	42.343	94.449
160.916	300.422	125.873	298.441	124.789	295.113
253.957	521.389	200.582	518.233	199.861	513.076

TABLE III. The lateral nearest-neighbor distance at multilayer coexistence.

T (K)	L_c (Å)				
	Bulk		Monolayer ^c	Bilayer ^d	Trilayer ^d
	Calculated ^a	Experiment ^b			
	CH ₄ (CD ₄)	CH ₄ (CD ₄)	CH ₄ (CD ₄)	CH ₄ (CD ₄)	CH ₄ (CD ₄)
0	4.083 (4.082)	4.148 (4.087)	4.285 (4.27)		
10		4.149 (4.088)	4.285 (4.28)	4.061 (4.053)	4.037 (4.030)
20		4.154 (4.093)	4.301 (4.29)	4.062 (4.055)	4.038 (4.031)
30		4.167 (4.139)	4.336 (4.32)	4.068 (4.059)	4.043 (4.037)
40		4.177 (4.153)	4.394 (4.37)	4.077 (4.072)	4.050 (4.046)
50		4.189 (4.166)	4.488 (4.44)	4.090 (4.085)	4.060 (4.056)
60		4.202 (4.183)	4.590 (4.54)	4.105 (4.101)	4.070 (4.067)

^aThis result is from the work of Bruch (Ref. 24).

^bExperimental results given by Aadsen and Simmons and co-workers (see Ref. 34).

^cThe equilibrium condition applied was zero spreading pressure.

^dThe results of applying the coexistence conditions Eqs. (6)–(8). The distance is the same for all layers within the given multilayer. The numbers in parentheses are for CD₄.

experiment. The lack of thermal expansion in the vertical direction is reasonable since the potential well is quite deep and narrow. The vertical well is nearly harmonic and the energy difference between the ground state and the first excited state is ~ 125 K at all temperatures. Indeed, considerable thermal energy must be added to the system before the first excited state is populated to any significant degree. A brief summary of typical energy eigenvalues is given in Table II.

The thermal expansion of the uncompressed (zero spreading pressure) monolayer is shown in Table III and the corresponding chemical potential is given in Table IV. At zero spreading pressure, the chemical potential is equal to the Helmholtz free energy. The lattice constants (Table III) and coexistence conditions satisfying Eqs. (6)–(8) are reported (Table IV). A graphical depiction of the solution for the coexistence conditions is given in Fig. 4. The plot of chemical potential with increasing spreading pressure

TABLE IV. The chemical potential and spreading pressure at multilayer coexistence.

T (K)	Monolayer ^a	Bilayer		Trilayer		Bulk ^b
	μ (K)	ϕ (K/Å ²)	μ (K)	ϕ (K/Å ²)	μ (K)	μ (K)
	CH ₄ (CD ₄)	CH ₄ (CD ₄)	CH ₄ (CD ₄)	CH ₄ (CD ₄)	CH ₄ (CD ₄)	CH ₄ (CD ₄)
0						−1030.5 (−1046.2)
10	−1886.1 (−1899.5)	50.12 (50.47)	−1133.3 (−1144.8)	57.20 (57.39)	−1079.8 (−1092.6)	
20	−1888.3 (−1902.3)	50.07 (50.41)	−1134.5 (−1146.5)	57.17 (57.30)	−1080.7 (−1094.0)	
30	−1896.0 (−1911.6)	49.86 (50.16)	−1140.5 (−1154.1)	57.05 (57.22)	−1085.9 (−1100.6)	
40	−1910.4 (−1928.2)	49.49 (49.74)	−1153.4 (−1169.2)	56.72 (56.83)	−1097.6 (−1114.7)	
50	−1931.7 (−1952.0)	48.99 (49.20)	−1172.4 (−1191.2)	56.50 (56.60)	−1114.4 (−1134.1)	
60	−1960.1 (−1983.1)	48.40 (48.59)	−1197.8 (−1219.4)	56.14 (56.20)	−1137.2 (−1159.9)	

^aThe monolayer values are for zero spreading pressure.

^bThis result is from Bruch (Ref. 24).

TABLE V. Lattice constants of the j layer at coexistence with a $j + 1$ layer.

T (K)	L_c (Å)	
	Monolayer lattice constant at monolayer bilayer coexistence	Bilayer lattice constant at bilayer trilayer coexistence
10	4.08	4.044
20	4.08	4.045
30	4.09	4.050
40	4.10	4.057
50	4.11	4.069
60	4.13	4.081

shows that below a critical spreading pressure the monolayer is a more stable structure than that of the bilayer. The same condition is also true for the bilayer-trilayer transition at a slightly higher pressure. From the data, it is clear that significant spreading pressures are required to compress a j layer to the point where a $(j + 1)$ layer is the more stable structure. It is interesting to note that the lattice constant of the monolayer at coexistence with the bilayer and for the bilayer at coexistence with the trilayer are, respectively, 0.02 and 0.01 Å larger than the corresponding lattice constant of the higher order multilayer (see Table V). The values for bulk CH_4 and CD_4 in Tables III and IV were calculated by Bruch³³ using both quantum-cell and the Hartree methods.

The latent heat of adsorption is an important thermodynamic property to calculate for this model, since it would be available in physical adsorption experiments. Latent heats of adsorption for the uncompressed monolayer and the bilayer at coexistence are given in Table VI for a range of temperatures [see Eqs. (9) and (10)]. The monolayer result q_1 and the bilayer result q_2 vary nearly 4 and 9%, respectively, over the temperature range (0–60 K).

The calculations described in Sec. IV are carried out in such a manner that the thermodynamic properties of individual layers within a bilayer or trilayer are computed separately. An unexpected result was noticed. If the lattice constant of an individual layer is determined by finding the minimum in the Helmholtz free energy (zero spreading pressure), the first layer has a significantly larger dilation than the upper layers. This is due to the greater repulsion experienced by the layer closest to the substrate surface from the MacLachlan interaction. The implications of a sizable misfit between successive layers could mean the existence of shearing stresses. If present, these stresses could be important in determining the modes of growth for multilayer systems. However, the rather high spreading pressures required to achieve coex-

istence are sufficient to compress the layers into commensurability with each other. Under these spreading pressures, the individual layers have nearly identical lattice constants. The bilayer and trilayer systems can be considered to move as a unit of two- and three-layer crystals with virtually no shear between layers.

VI. DISCUSSION

The calculations reported in this paper represent an attempt to determine the thermodynamic and structural properties of an intermolecular interaction model over the full range of temperatures corresponding to stable solid films. I have used the quantum-cell model for the statistical mechanics which includes fully the anharmonic nature of the potentials and the quantum-mechanical effects. These extensions are needed to quantitatively describe the properties of the methane on graphite system over such a wide range of temperatures. The intention is to move closer to direct comparisons with experiment than the valuable models for multilayer films based on static lattice sums by Muirhead *et al.* and Gittes and Schick.¹ Bruch and co-workers^{2,24} have already extended the discussion in the current literature by the addition of zero-point effects and realistic potentials.

The agreement between previous theories of multilayer growth with experiment is quite good for argon, krypton, and xenon adsorbed on graphite. However, there have been conflicting comparisons for other systems (neon and methane) which would appear to be in the same general class. Insofar as the general mode of multilayer growth is indicated in the construction of the first three layers, the determination of the properties of the methane on graphite gives some insight into the nature of the systems near the crossover between wetting and partial wetting.

Any empirical model of a system as complicated as methane on graphite will be less than precise when compared with very accurate experimental measurements. The best that can be reasonably expected is that calculated

TABLE VI. Heat of adsorption. This data has not been corrected for the librational kinetic energy; subtract approximately 105 K/molecule.

T (K)	q_1 (K/molecule)	q_2 (K/molecule)
	Heat of adsorption for an uncompressed monolayer	Heat of adsorption for a bilayer at monolayer/bilayer coexistence
10	1927	1186
30	1983	1241
60	2008	1302

results will be within the range of values given by different experiments. This appears to be the case for most properties where comparisons can be made. When considering small absolute differences in calculated values that are less than a reasonable uncertainty to experiment, comparisons should be made internal to the model. For example, in film to bulk comparisons, film values of chemical potential should be compared with bulk values calculated with the same model under the approximations.

Two of the more useful properties for direct comparison of theory to experiment are structure and heats of formation. The ground-state lattice constants bulk CH_4 and CD_4 calculated by Bruch for this model and the very precise experiments of Simmons and co-workers³⁴ show the model to predict a value nearly 1.5% too low for CH_4 and very close for CD_4 . The agreement, particularly for CD_4 , cannot be taken literally because of an orientational phase transition that is not built into the model calculation. The thermal expansion of the monolayer was shown to compare well with experiment in paper I.⁶ The model was the first to predict the $\sqrt{3} \times \sqrt{3}$ registry observed in a number of experiments (see the references in paper I). The model also predicts the commensurate-incommensurate transition temperature of the monolayer fairly well. The height of the monolayer above the graphite is within the experimental limits. The lack of any significant thermal expansion in the vertical direction would be very difficult to test experimentally. The thermal expansion of solid bilayer and trilayer films at their coexistence conditions (see Tables IV and V) could be testable, providing the formidable experimental difficulties can be overcome.

The heat of adsorption is an important experimental result and a good test of the energetics of any quantitative interaction model. Recent experiments by Gay *et al.*³¹ show quite reasonable comparisons to the results of this calculation. The correspondence between the experimental values and the theoretical predictions indicates the methane-methane and methane-graphite interaction parameters to be an acceptable scaling of the physical system.

Gay *et al.*³¹ estimate from their data that the heat of adsorption for the uncompressed monolayer solid is 4.0 kcal/mole (2013 K/molecule) at 67 K. My calculated value, at 60 K, is $q_1 = 1903.2$ K/molecule (3.78 kcal/mole). An estimate of 105 K/molecule for the librational kinetic energy¹⁴ has been subtracted from the quantum-cell-model result. If $4 \Delta T$ is added to the calculated value to compensate for the temperature difference, the calculated value is 4% below the experimental estimate. The difference between the isosteric heat and the heat of adsorption of a solid monolayer at three-phase coexistence, $q_{st} - q_1$, is a measure of the contribution of the lateral interactions in the monolayer. By using Eq. (11), the calculated difference is 364 K/molecule (0.72 kcal/mole) and the experimental result³¹ is 0.7 kcal/mole (352 K/molecule). The vertical contribution to the internal energy is reported by Gay *et al.*³¹ to be 3.3 kcal/mole (1661 K/molecule) and the corresponding calculation gives 1580 K/molecule (3.14 kcal/mole) for a 5% comparison.

The values for solid bilayer heats of adsorption at coexistence are given in Table VI. With the extensive activity being done on multilayer systems, future experiments may provide data for comparisons for the bilayer and trilayer systems. Very recently, the bilayer and trilayer isosteric heats of adsorption ($35 < T < 40$ K) have been measured to be 2.37 ± 0.2 and 2.47 ± 0.2 (kcal/mole), respectively.³⁵ From Table VI, the bilayer heat of adsorption is $(1241 - 105) = 1136$ K/molecule (2.26 kcal/mole).

An important feature of this calculation is that the statistical mechanics has been carried out in such a manner that the properties of each layer within the bilayer or trilayer are known individually. Due to the substrate mediated MacLachlan interaction, which is basically repulsive, the lattice constants of unconstrained individual layers differ significantly. In the bilayer, the lattice constant of the first layer closest to the substrate is 2% larger than that of the second layer. The spreading pressure is allowed to increase to the value required by Eqs. (6) and (7) for coexistence. Then the lower layer, being more compressible, easily breaks its registry with the graphite substrate and compresses 5% to the values shown in Table III. The second layer has compressed to within 0.01 Å of the first-layer lattice constant. Since the amplitude of the undulation of the graphite of the graphite substrate is more than an order of magnitude less than that which the second layer experiences due to the first layer, the layers were quantitatively shown to be locked together and compress as a two-layer crystal to the equilibrium configuration (see Table IV and Fig. 1). The trilayer system follows the same structural path to coexistence. The bilayer and trilayer systems for CH_4 and CD_4 have been studied over the temperature range (0–60 K) and the above description is followed in each case.

Informally, the question of whether shearing stresses exist between adjacent layers has often been raised. These calculations clearly show that under coexistence conditions, the shear effects are not present. It should be noted, however, that in the system considered, the periodic substrate has an amplitude considerably smaller than the one internal to the adsorbate. This supports an assumption made by Gittes and Schick¹ in their potential energy model—the individual layers within the film are in registry with each other.

It is important to place this calculation in context with other recent calculations on thick films, long-range forces, and wetting.^{36,7,37} The differences center on the Bruch criteria for coexistence [Eqs. (6) and (7)]. The completion of a very thin multilayer depends upon reaching a particular value of chemical potential by increasing the spreading pressure work term. This implies that all layers in the thin multilayer (2 or 3) are experiencing the same “2D-gas” compression. If the multilayer is very thick, the top layers experience only the more dispersed 3D-gas pressure. This difference in compressive forces experienced by the lowest (next to the substrate) and the highest layers within the film, gives rise to elastic strains in the intervening layers.^{36,7} According to Huse³⁶ the strain falls off at long distances $\sim z^{-3}$. Should the strain energy at any height exceed the threshold for dislocation formation, the film becomes unstable in this respect.

The Bruch criteria and this calculation assume a uniform spreading pressure with height z . Therefore, the consequences are true only for very thin films (here, three layers). If this calculation were applied to thick films, the Bruch criteria for coexistence would need to be modified to take into account the role of the changing compression with height above the substrate. The change is due to the lateral effects from the spreading pressure at the substrate to the 3D-gas pressure acting on the top layers.

There does not appear to be any fundamental disagreement between these bilayer and trilayer results via QCT and the formal points raised in Huse,³⁶ Gittes and Schick,⁷ and Nightingale *et al.*³⁷ The place of this model may be viewed as a microscopic picture of the thin-film limit of the models of Huse³⁶ and Gittes and Schick.⁷ The model can represent the behavior of highly compressed films of a few layers. This calculation will hopefully be close to representing the experimental situation.

The most significant result of this research is the implications it carries for the modes of multilayer growth. Insofar as the type of growth mode that may possibly be set in the buildup of the first three layers, the data given in Tables III and IV give some insight into the changing discussion between experiment and theory. For systems which scale to the regime of methane or neon on graphite and for temperatures below the 2D triple line, there are sizable quantum and anharmonic effects. The quantum-cell model is a natural choice to calculate realistic values for the Helmholtz free energy and the internal energy. From these results, the spreading pressures and chemical potentials are derived. The solutions to the coexistence conditions, Eqs. (6) and (7), given in Tables III and IV, show the bilayer and trilayer to be overcompressed, i.e., the lattice constant is less than that of the 3D bulk crystal. The lattice constant of the bilayer is compressed $\frac{1}{2}\%$ and the trilayer is 1% smaller than the corresponding bulk. However, the chemical potential is still below that of the bulk. The climb of the chemical potential from the uncompressed solid monolayer to the bilayer and trilayer at coexistence occurs in successive jumps of 753 K/molecule, 53.5 K/molecule, respectively. The trilayer at coexistence is still 49.3 K/molecule below the 3D bulk value calculated for the same model. If the calculated 3D results scale up in temperature in the same fashion as the experimental data of Simmons and co-workers,³⁴ the circumstances do not appear to differ significantly for all the temperatures below the 2D triple line.

Goodstein *et al.*³⁸ report that the monolayer condenses at 725 K/molecule and the bilayer 80 K/molecule below the bulk. Presumably, the values are measured above 65 K. The results given in Table IV give these same differences to be 856 and 102.8 K/molecule, respectively, for the ground state. The comparison is quite reasonable considering the differences in the temperatures.

Note also that the spreading pressure required to achieve coexistence is five times the spreading pressure needed to drive the monolayer out of the $\sqrt{3} \times \sqrt{3}$ registry and incommensurate with the graphite.⁶ It would appear that the substrate periodicity has little to do with the mode of multilayer growth for the methane on graphite

system.

The experimental situation is a difficult one. The films are overcompressed by the spreading pressure to the point where the lattice constant is less than in 3D bulk but the chemical potential is still 50 K/molecule below the bulk. Clearly, any slight imperfections or defects (heterogeneities) which could raise the chemical potential would become growth sites for 3D crystallites. Such an occurrence experimentally could very easily be interpreted as a case of partial or incomplete wetting (type 2). Growing 3D single crystals of methane require extreme care and very long preparation times (see Aadsen³⁴). It should not be surprising that the observation of solid bilayers and trilayers of methane on graphite at temperatures below the 2D triple line has been difficult. Gay *et al.*³¹ show in their Fig. 4, among other properties, lines for the condensation of multilayers at low temperatures. They leave the discussion of these experiments to a later publication. At higher temperatures, Hamilton and Goodstein³⁸ and Piper and Morrison³⁹ have reported the growth of methane multilayers on graphite.

In summary, the potential parameters used for these calculations in describing the adsorbate-adsorbate and the adsorbate-substrate interactions work sufficiently well to make meaningful comparisons to experimental data. MacLachlan substrate-mediated forces are again needed to complete the model. The quantum-mechanical cell model accounts for the quantum-mechanical and the large anharmonic effects very well.

Both structural properties and heats predicted by the model are within reasonable limits of a variety of experiments. The role of periodicity in the substrate potential does not enter significantly into the process of multilayer growth. The strength, range, and z dependence of the substrate potential would appear to be the determinative factors. Rotational transitions at low temperatures are not fully investigated by the model, but the energetics involved suggest that the details may not be important. Shearing strains do not appear to exist between individual layers within a multilayer film.

The overcompression of the bilayer and trilayer films at coexistence and the close approach of the chemical potential to that of bulk may well be part of the reason for disagreements between theory and early experiments. Recent experiments^{31,38,39} appear to be more in line with the predictions of this model. In order for there to be direct comparisons, more experiments need to be done at low temperatures and the calculations need to be done for higher temperatures.

ACKNOWLEDGMENTS

I wish to thank Professor L. W. Bruch for helpful discussions and especially for the use of his calculations of the 3D bulk properties. I also thank J. Gay, J. Krim, J. Suzanne, E. L. Lerner, and A. Dutheil for their data prior to publication. Acknowledgment is made to the Donors of The Petroleum Research Fund, administered by the American Chemical Society, for the support of this research.

- ¹R. J. Muirhead, J. G. Dash, and J. Krim, *Phys. Rev. B* **29**, 5074 (1984); F. T. Gittes and M. Schick, *ibid.* **30**, 209 (1984).
- ²L. W. Bruch and X.-Z. Ni, *Faraday Discussion No. 80*, edited by J. A. Morrison, Vol. 80 (to be published).
- ³Jacqueline Krim, Ph.D. thesis, University of Washington, 1984; J. G. Dash, *Phys. Today* **38**, (12) 26 (1985); M. Bienfait, *Surf. Sci.* **162**, 411 (1985); R. Pandit, M. Schick, and M. Wortis, *Phys. Rev. B* **26**, 5112 (1982); M. P. Nightingale, W. F. Saam, and M. Schick, *Phys. Rev. Lett.* **51**, 1275 (1983); C. Ebner, C. Rottman, and M. Wortis, *Phys. Rev. B* **28**, 4186 (1983).
- ⁴L. W. Bruch and M. S. Wei, *Surf. Sci.* **100**, 481 (1980); M. W. Wei and L. W. Bruch, *J. Chem. Phys.* **75**, 4130 (1981).
- ⁵L. W. Bruch, J. M. Phillips, and X.-Z. Ni, *Surf. Sci.* **136**, 361 (1984); also see Ref. 2.
- ⁶James M. Phillips, *Phys. Rev. B* **29**, 4821 (1985); **29**, 5865 (1984) (paper II); James M. Phillips and M. D. Hammerbacher, *Phys. Rev. B* **29**, 5859 (1984) (paper I).
- ⁷F. T. Gittes and M. Schick, *Phys. Rev. B* **30**, 209 (1984).
- ⁸L. W. Bruch and J. M. Phillips, *Surf. Sci.* **91**, 1 (1980).
- ⁹J. A. Barker, in *Rare Gas Solids*, edited by M. L. Klein and J. A. Venables (Academic, London, 1976), Vol. I, Chap. 6.
- ¹⁰R. A. Aziz, in *Inert Gases*, edited by M. L. Klein (Springer-Verlag, Berlin, 1984), Chap. 2.
- ¹¹D. E. Williams, *J. Chem. Phys.* **45**, 3770 (1966); **47**, 4680 (1967); A. I. Kitaigorodskii, *Tetrahedron* **9**, 183 (1960); A. I. Kitaigorodskii, *Molecular Crystals and Molecules* (Academic, New York, 1973); R. O. Watts and I. J. McGee, *Liquid State Chemical Physics* (Wiley-Interscience, New York, 1976).
- ¹²E. S. Severin and D. J. Tildesley, *Mol. Phys.* **41**, 1401 (1980).
- ¹³S. F. O'Shea and M. L. Klein, *J. Chem. Phys.* **71**, 2399 (1979).
- ¹⁴R. Righini, K. Maki, and M. L. Klein, *Chem. Phys. Lett.* **80**, 301 (1981).
- ¹⁵W. A. Steele, *J. Phys. Chem.* **82**, 817 (1978).
- ¹⁶W. A. Steele, *The Interaction of Gases with Solid Surfaces* (Pergamon, Oxford, 1974).
- ¹⁷L. W. Bruch, *Surf. Sci.* **125**, 194 (1983).
- ¹⁸A. D. MacLachlan, *Mol. Phys.* **7**, 381 (1964).
- ¹⁹S. Rauber, J. R. Klein, M. W. Cole, and L. W. Bruch, *Surf. Sci.* **123**, 173 (1982).
- ²⁰D. J. Margoliash, T. R. Proctor, G. D. Zeiss, and W. J. Meath, *Mol. Phys.* **35**, 747 (1978).
- ²¹J. M. Phillips and L. W. Bruch, *J. Chem. Phys.* **79**, 6282 (1983); L. W. Bruch, J. M. Phillips, and X.-Z. Ni, *Surf. Sci.* **136**, 361 (1984); L. W. Bruch and J. M. Phillips, *J. Phys. Chem.* **86**, 1146 (1982).
- ²²J. O. Hirschfelder, C. F. Curtiss, and R. B. Bird, *Molecular Theory of Gases and Liquids* (Wiley, New York, 1954).
- ²³J. L. Seguin, J. Suzanne, M. Bienfait, J. G. Dash, and J. A. Venables, *Phys. Rev. Lett.* **51**, 122 (1983).
- ²⁴L. W. Bruch (private communication); also see Refs. 2 and 5.
- ²⁵J. M. Phillips and L. W. Bruch, *Surf. Sci.* **81**, 109 (1979); J. M. Phillips, L. W. Bruch, and R. D. Murphy, *J. Chem. Phys.* **75**, 5097 (1981).
- ²⁶J. A. Barker, *Lattice Theories of the Liquid State* (MacMillan, New York, 1963).
- ²⁷A. C. Holt, W. G. Hoover, S. G. Gray, and D. R. Shortle, *Physica* **49**, 61 (1970).
- ²⁸J. M. Phillips, L. W. Bruch, and R. D. Murphy, *J. Chem. Phys.* **75**, 5097 (1981).
- ²⁹J. A. Barker, *J. Chem. Phys.* **44**, 4212 (1966); J. A. Barker and E. R. Cowley, *ibid.* **73**, 3452 (1980).
- ³⁰B. L. Holian, *Phys. Rev. B* **22**, 1394 (1980).
- ³¹J. M. Gay, A. Dutheil, J. Krim, and J. Suzanne (unpublished).
- ³²R. Marx and E. F. Wasserman, *Surf. Sci.* **117**, 267 (1982).
- ³³L. W. Bruch (private communication).
- ³⁴D. R. Aadsen, Ph.D. thesis, University of Illinois (1975); D. R. Baer, B. A. Fraass, D. H. Riehl, and R. O. Simmons, *J. Chem. Phys.* **68**, 1411 (1978).
- ³⁵J. Krim, J. M. Gay, J. Suzanne, and E. Lerner (private communication).
- ³⁶D. A. Huse, *Phys. Rev. B* **29**, 6985 (1984).
- ³⁷M. P. Nightingale, W. F. Saam, and M. Schick, *Phys. Rev. Lett.* **51**, 1275 (1983); M. P. Nightingale, W. F. Saam, and M. Schick, *Phys. Rev. B* **30**, 3830 (1984).
- ³⁸D. L. Goodstein, J. J. Hamilton, M. J. Lysek, and G. Vidali, *Surf. Sci.* **148**, 187 (1984); J. J. Hamilton and D. L. Goodstein, *Phys. Rev. B* **28**, 3838 (1983).
- ³⁹J. Piper and J. A. Morrison, *Phys. Rev. B* **30**, 3486 (1984).